Spring 5-2020

Glutamine Antagonist 6-diazo-5-oxo-L-norleucine, a Hyaluronan Synthesis Inhibitor, Slows Triple Negative Breast Cancer Growth

Le Gia Cat Pham
University at Albany, State University of New York, cpham@albany.edu

Glutamine Antagonist 6-diazo-5-oxo-L-norleucine, a Hyaluronan Synthesis Inhibitor, Slows Triple Negative Breast Cancer Growth

An honors thesis presented to the
Department of Biomedical Sciences
University at Albany, State University of New York
in partial fulfillment of the requirements
for graduation with Honors in Bioinstrumentation
and
graduation from The Honors College

Le Gia Cat Pham

Research Advisor: JoEllen Welsh, Ph.D.
Second Reader: Carmen J. Narvaez, Ph.D.

May 2020

Abstract

Triple-negative breast cancers (TNBC) are the most aggressive subtype of breast cancer with few treatment options and poor outcomes. TNBCs are characterized by elevations in hexosamine biosynthetic pathway (HBP) enzyme expression, hyaluronan synthase 2 (HAS2) expression and hyaluronan (HA) production. Glutamine is an important substrate for HA production via the HBP. 6-diazo-5-oxo-L-norleucine (DON) is a well-known glutamine antagonist with validated antitumoral efficacy. This project examined the effects of DON on HA production and energy metabolism in TNBC cells. We examined the effect of DON treatment on Hs578T cells, which represent the mesenchymal stem-like subtype of TNBC. We specifically analyzed the effects of DON on Hs578T cell variants segregated into high (HA^{High}) and low (HA^{Low}) HA producing subpopulations. DON decreased cell proliferation in both cell lines with HA^{Low} cells showing a more pronounced effect with almost 40% decrease in cell number after treatment with 2.5μM DON for 72 hours. DON reduced cell-associated HA in a dose dependent manner in HA^{High} cells whereas HA^{Low} cells exhibited no effect. Seahorse extracellular flux analysis indicated that HA^{High} cells were more sensitive to DON with about 60% decrease in glycolysis compared to an almost 40% decrease in HA^{Low} cells. The observed changes in glycolysis and reduction in HA production in HA^{High} cells support the findings that DON can inhibit glutamine dependent enzymes in HBP and hinder tumor growth in TNBC cells.

Acknowledgements

I am grateful to my academic and research advisor Dr. JoEllen Welsh. She has provided me the opportunity and all the means for undergraduate research. My experience in the lab with wonderful people strengthened my knowledge about Biological Sciences and would lead me to greater heights. I am grateful for Dr. Carmen J. Narvaez's guidance with my research works. I also want to express my greatest gratitude to Dr. Martin Tenniswood for his judicious counseling.

List of figures

Table of Contents

Introduction

Healthy breast epithelial cells receive messages from hormones (estrogen and progesterone) to maintain functions and proliferate as needed (ie, during puberty or pregnancy). Cell growth is also regulated by HER2, a growth factor receptor often up-regulated in breast cancers. High activity of HER2 or the receptors for estrogen and progesterone drive breast cancer growth and thus represent therapeutic drug targets. Therapies targeting the effects of these hormones and HER2 effectively slow and even stop the growth of breast cancers that express these proteins. Triple-negative breast cancer (TNBC) refers to breast cancers that do not express the estrogen receptor (ER), progesterone receptor (PR) or HER2 (Foulkes et al., 2010). Triple-negative tumors comprise 15-20% of breast cancers, mostly women with mutations in the BRCA1 gene (Perou, 2011). Since hormones or HER2 do not fuel their growth, TNBCs are more difficult to treat and often require combination therapies. Although some data suggest that chemotherapies have better effects on TNBC than other types of breast cancer, overall, prognosis for these patients remains poor (De Giorgi et al., 2007). As a result, TNBC has a more aggressive metastatic nature, and shorter adjuvant and neoadjuvant disease-free period.

Many tumors alter critical biochemical pathways to enhance nutrient supply for rapid growth. These changes can affect cellular metabolism and induce cellular stress (Wellen et al., 2010). During normal cell growth, glucose and glutamine are the primary substrates for energy and biosynthesis of macromolecules for cell proliferation. Cancer cells often undergo a "metabolic switch" from mitochondrial respiration to glycolysis even when oxygen is available (Warburg et al., 1927). The hexosamine biosynthetic pathway (HBP, ***Figure 1***) is another key

regulator of tumor promotion as it metabolizes glucose and glutamine to hexoses that can be incorporated into hyaluronic acid (HA), a glycan associated with aggressive tumors.

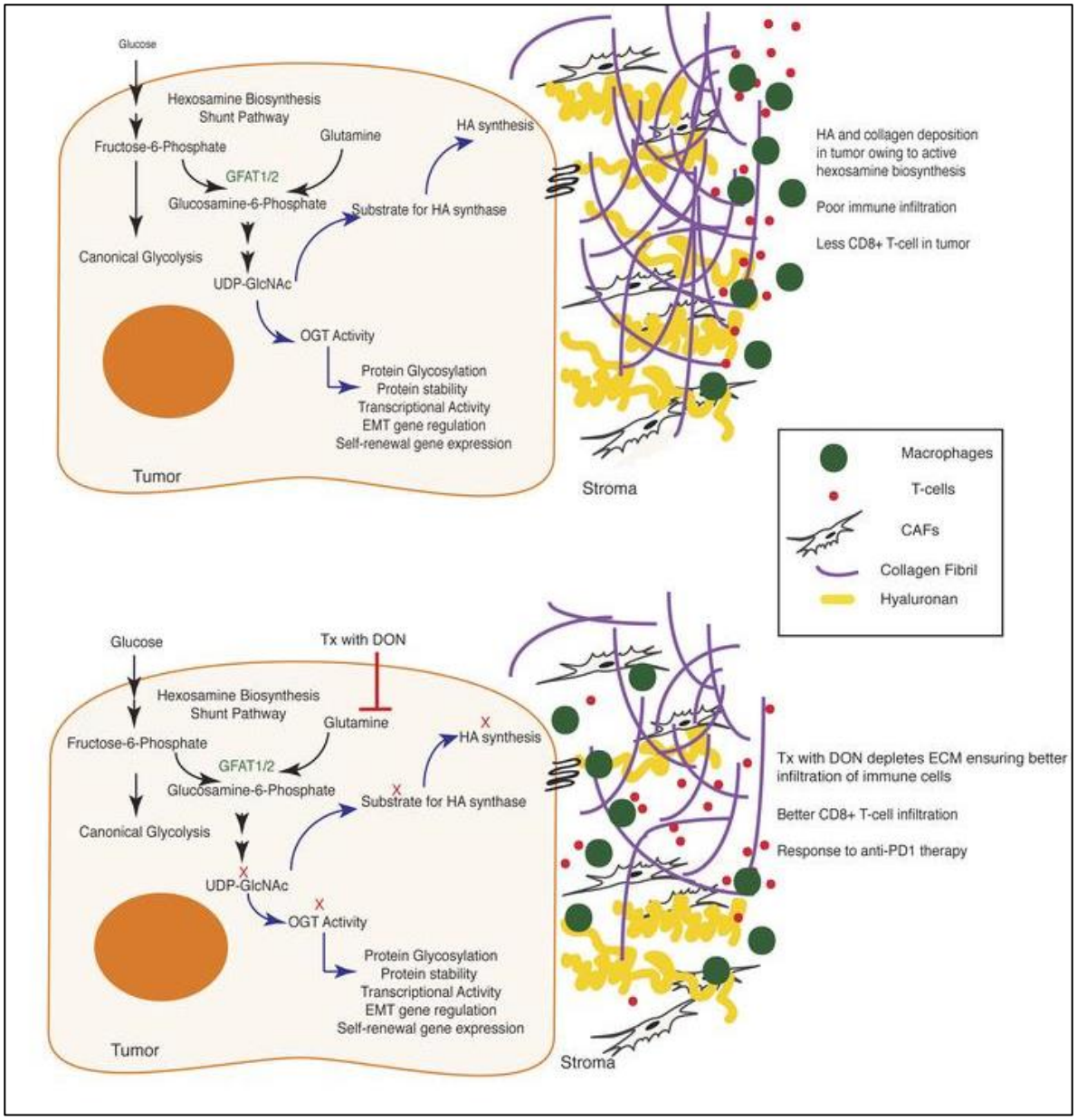

Figure 1. Effects of DON on hexosamine biosynthetic pathway (HBP) in pancreatic tumors (Sharma et al., 2019). The cell takes in glucose, processes it through a two-step conversion to fructose-6P. After that, 95% of fructose-6p goes to glycolysis and around 5% goes through glucosamine-6P conversion by GFAT (glutamine: fructose-6-phosphate amidotransferase) with the aid of glutamine that cell took in. GFAT is the rate-limiting enzyme for the formation of hexosamine products and acts as a key regulator of HBP. GNA1/GNPNAT1 helps convert glucosamine-6P into GlcNAc-6P using acetyl-CoA from fatty acid metabolism. PGM3/AGM1 then catalyze the conversion to GlcNAc-1P. UDP-GlcNAc is synthesized by UAP/AGX1 using UTP from the nucleotide metabolism pathway. N-linked and O-linked glycosylation in ER and Golgi occurred for O-GlcNAc modification of nuclear and cytoplasmic proteins

The end products of the HBP, UDP-N-aceytylglucosamine (UDP-GlcNAc) and UDP-glucuronic acid (UDP-GlcUA) are essential substrates for HA synthesis (Vigetti et al., 2012). Analyses of breast cancer mouse models indicated HBP enzyme expression in carcinoma cells, with higher expression of Hyaluronan synthase 2 (HAS2) and higher HA production in aggressive breast cancer cells (Chokchaitaweesuk et al., 2019). As noted above, independent from the HBP, glutamine is also required for the production of glutamate (catalyzed by glutaminase and glutamine amidotransferase enzymes). Glutamate is thus important for HA synthesis, the mitochondrial tricarboxylic acid cycle (TCA cycle) and cellular energy production.

6-diazo-5-oxo-L-norleucine (DON) is a glutamine antagonist with antitumoral efficacy as validated in various models (Yoshioka et al., 1992). DON can bind active sites of glutamine metabolic enzymes, such as GFAT in the HBP, and inhibit them by alkylation (Ortlund et al., 2000). In vitro, DON treatment results in apoptosis through the disruption of mitochondria metabolism (Wu et al., 1999).

This project studied the effects of DON on HA production and other relevant glutamine metabolic pathways in TNBC. Hs578T is an established human cell line that is representative of the mesenchymal stem-like subtype of TNBC. We hypothesized that DON treatment would have different effects on sub-populations of Hs578T cell lines that synthesize high or low amounts of HA. To test this hypothesis, parental Hs578T cells were sorted by flow cytometry into HA^{High} and HA^{Low} populations. The HA^{High} subclone demonstrated more aggressive properties, elevated HA production, and overexpression of enzymes that metabolize glucose and glutamine. We analyzed the impact of DON treatment on HA^{High} and HA^{Low} cell growth with crystal violet assays and detected a pronounced effect at 2.5 μM DON treatment. Higher concentrations of DON with a shorter time point were utilized in the following experiments. Flow cytometry of

bHABP binding to cell-associated HA on subpopulations was performed after treatment with 5 and 10 μM DON for 48 hours. We also characterized the effect of 24 hour treatment with 5 μM DON on metabolism (Mitochondrial Function and Glycolytic Function) of the subpopulations using the Agilent Seahorse XFp Analyzer.

Materials and Methods

Cell Culture

Hs578T cells, a triple-negative breast cancer (TNBC) cell line, was originally obtained from ATCC and was available in the Welsh lab. This "parental" cell line was sorted into High (HA^{High}) and Low (HA^{Low}) HA populations by flow cytometry after incubation with biotinylated hyaluronic acid binding protein (bHABP) which binds to cell-associated HA. The resulting subclones were grown in Dulbecco's Modified Eagle Medium with high glucose (DMEM), 10% fetal bovine serum (FBS), 15nM HEPES and 10 µg/mL insulin. Cells were cultured every 4-5 days at the density of 4,000 cells/cm2, with media replaced every 2 or 3 days, and kept in an incubator at 5% CO2 and 37°C.

Cell Morphology - Confocal microscopy

Lab-Tek II CC2 4-well chamber slides were used to plate Hs578T subclones with 5,000 cells/cm2 for 72 h. 1% formaldehyde in PBS was used to fix cells for 15 minutes and PBS/1% BSA containing 0.02% sodium azide was used to block overnight. bHABP was diluted 1:30 in blocking buffer. The cells were incubated in the dilution for 30 minutes at room temperature in a humidified chamber. After the incubation period, the chamber slides were washed with PBS 3 times. The slides were incubated with Alexa Fluor 488 streptavidin diluted 1:400 in blocking buffer. After three washes with PBS, coverslips were applied with Invitrogen Prolong Gold antifade mounting media containing DAPI to identify nuclei. Images were taken with a 40x oil immersion objective on a Leica DMI6000 microscope with TCS SP5 confocal laser scanner using Leica Application Suite AF version 2.6.0.7266 software.

Particle exclusion assay

Lab-Tek II 4-well chambered coverglass #1.5 borosilicate was used to plate Hs578T subclones with 500 cells/cm2 density for 48h. The cells were rinsed with Sigma Hank's Balanced salt solution, fixed for 10 min in 1% formaldehyde in HBSS at room temperature, washed three times with HBSS, and incubated for 15 min with Hoechst 33258 diluted 1:150 in PBS/0.2% BSA. The cells were washed three times with PBS/0.2% BSA, after which 7.5 x 10^8 fixed sheep red blood cells were overlaid onto cultures and allowed to settle for 20 min at 37°C. Images were taken with a 20x objective on the Leica DMI6000 confocal microscope.

Crystal Violet Assay

A simple method used to determine cell survival and growth is based on the use of crystal violet dye which binds to proteins and DNA, thus staining adherent cells in the culture (Feoktistova et al., 2016). This assay quantitatively assesses the density of cells which reflects both proliferation and cell death (apoptosis). Cells which lose the ability to attach to the substrate (including adherent cells triggered to undergo cell death) are not stained by the dye, decreasing the intensity of crystal violet staining. The crystal violet assay was applied to test the effect of DON on Hs578T HA^{High} and HA^{Low} subclones. The subclones were plated on 24-well dishes at 7,000 cells/ml density and treated with 0 µM, 0.5 µM, 1 µM, or 2.5 µM DON for 72 hours. After being fixed, washed, stained with crystal violet, and dried overnight, Triton X-100 was added to resuspend the dye. Plates were incubated for 30 minutes after which absorbance at 590nm was measured using a Victor microplate reader.

bHABP Flow Cytometry

Hs578T subclones were plated in 100mm^3 dishes (20,000 cells/mL) for one day. The subclones were incubated in respective treatments (5 µM DON, 10 µM DON) for 48 hours. The cells were trypsinized and pooled. Thereafter, all steps were performed at 4°C. The pooled cell suspension was blocked with PBS/4% BSA, incubated for 30 min with biotinylated HA binding protein (bHABP) diluted 1:30 in blocking buffer, and fluorescently labeled for 15 min with Alexa Fluor 488 streptavidin diluted 1:800 in blocking buffer. PBS/0.2% BSA was used for washes to remove unbound bHABP and streptavidin. Flow cytometry was performed on a BD LSR II Flow Cytometer and data was analyzed with FlowJo 7.6.5.

Measuring Glycolytic Function

Agilent Seahorse XFp Analyzer was used to measure glycolytic function in Hs578T HA^{High} and HA^{Low} cells after 24 h incubation in 5µM DON. Cells were plated in Seahorse 8-well XFp cell culture microplates at 6,000 cells/well density in triplicate. For each replicate, 3 wells were treated with 5µM DON and 3 wells were untreated. Cells were switched to buffer-free XF assay media (Agilent Seahorse) containing 2mM glutamine one hour prior to assay. The Agilent Seahorse XFp Cell Glycolysis Stress Test measures key parameters of glycolytic function by directly measuring the extracellular acidification rate (ECAR). Seahorse XFp Analyzer measures ECAR in real-time of the 3 replicates through injections of glucose, Oligomycin, and 2-DG. After the plates were measured, cells in each well were sonicated. The data from the 3 replicates were normalized with the DNA concentration in each well, measured by NanoDrop™ 2000/2000c Spectrophotometers.

Measuring Mitochondrial Function

The Agilent Seahorse XFp Analyzer was used to measure mitochondrial function in Hs578T HA^{High} cells after 24 h incubation with 5µM DON. Cells were plated in Seahorse 8-well XFp cell culture microplates at 6,000 cells/well in triplicate. For each replicate, 3 wells were treated with 5µM DON and 3 wells were left untreated. Cells were switched to buffer-free XF assay media (Agilent Seahorse) containing 1 mM pyruvate, 25 mM glucose with 2mM glutamine one hour prior to assay. The Agilent Seahorse XFp Cell Mito Stress Test measures key parameters of mitochondrial function by directly measuring the oxygen consumption rate (OCR) of live cells. Seahorse XFp Analyzer measures OCR in real-time of the 3 replicates through injections of Oligomycin, FCCP, Rotenone, and Antimycin. After the plates were measured, cells in each well were sonicated. The data from the 3 replicates were normalized with the DNA concentration in each well, measured by NanoDrop™ 2000/2000c Spectrophotometers.

Results

Cell morphology of high and low HA producing Hs578T subclones

Representative phase contrast images of HA^{High} and HA^{Low} cultures are shown in ***Figure 2A.*** A clear distinction in cell morphology was observed, with HA^{High} cells demonstrating fibroblastic features (spindle shaped) and HA^{Low} cells exhibiting epithelial morphology (cuboidal). At high density, the HA^{Low} cells grew as flat monolayers and were larger than the HA^{High} cells. Thus, sorting Hs578T cells for HA production separated the two morphological types of cells which were evident in the parental strain.

The differences in morphology and HA production in the two cell lines were verified with immunofluorescence and particle exclusion assays. Confocal imaging with bHABP showed more intense surface HA staining in the HA^{High} population than the HA^{Low} population (***Figure 2B***, Left). To specifically visualize the pericellular matrix, or cell coat, which is mostly comprised of cell surface HA anchored via HA synthases and HA-binding proteins (Tamada et al., 2012), we conducted particle exclusion assays. This technique utilizes sedimenting fixed erythrocytes (which are inherently fluorescent) to outline the edges of the pericellular matrix. Consistent with confocal imaging demonstrating extensive cell surface bHABP in the HA^{High} population, these cells had a more extensive pericellular coat than the HA^{Low} population (***Figure 2B***, Right). Phase contrast imaging of the low-density cultures used for the particle exclusion assay highlighted the smaller overall size and pronounced surface protrusions of the HA^{High} cells compared to the HA^{Low} cells.

A.

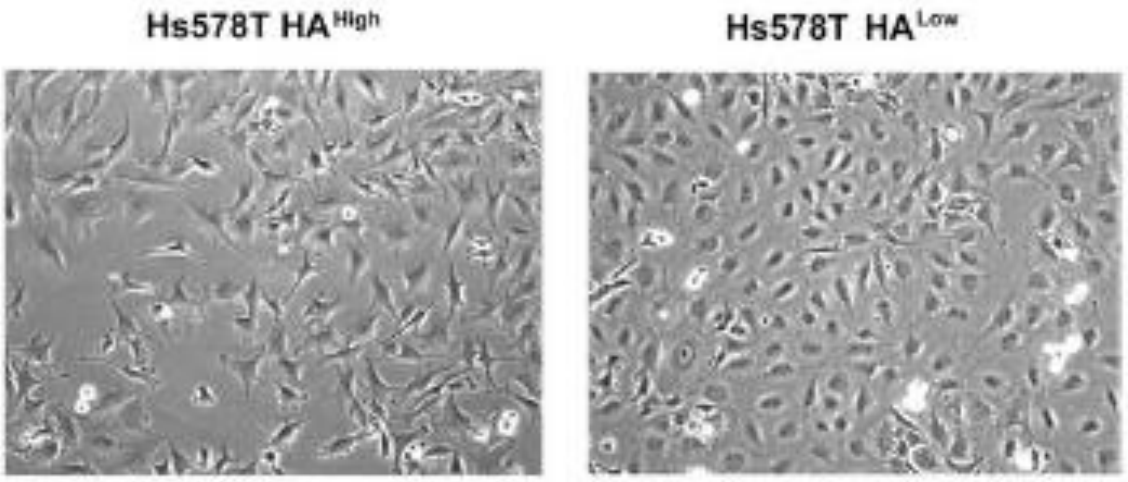

B.

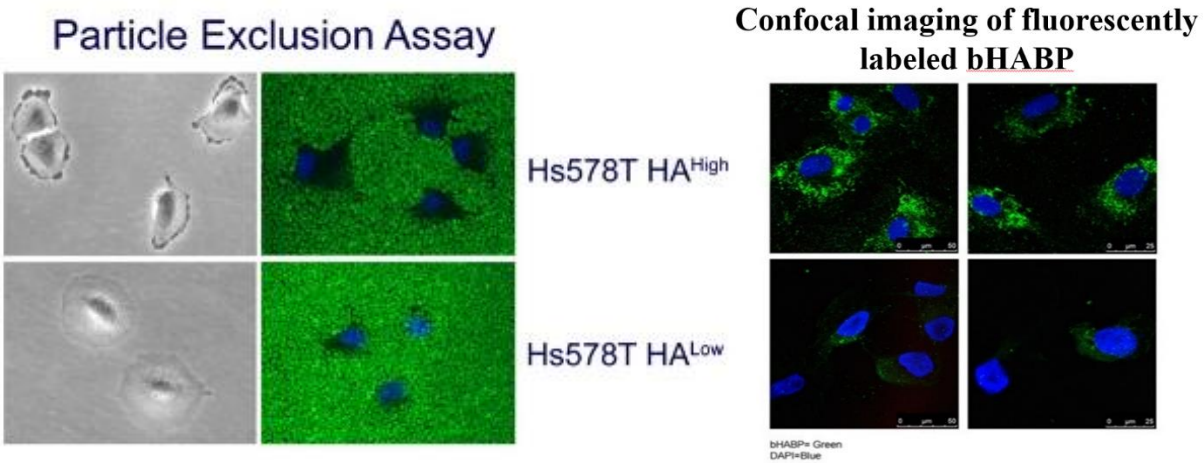

Figure 2. Morphology and HA expression of Hs578T subclones. **A**. Phase images of HAHigh and HALow subclones. **B.** Right: Confocal imaging of fluorescently labeled bHABP binding to cell-associated HA on Hs578T subclones. Left: Phase images and visualization of pericellular HA coat by exclusion of sedimenting fixed erythrocytes on Hs578T subclones**.**

Effects of DON on Hs578T subclones growth

Crystal violet assays were used to assess the dose dependent effect of DON on Hs578T HA^{High} and HA^{Low} subclones. Absorbance at 590nm in each well was recorded on a Victor microplate reader. The values for each treatment group were compared to that of the control wells and expressed as the percentage of the average absorbance (mean ± standard deviation).

For HA^{Low} cells, the average absorbance at each DON dose 98.0±8.4% at 0.5 µM, 83.2 ± 4.6% at 1 µM and 61.7 ± 1.2%. at 2.5 µM. For HA^{High} cells, the average absorbance at each DON dose was 95.9±5.9% at 0.5 µM, 87.4 ± 3.0% at 1 µM and, 71.3 ± 1.4%. at 2.5 µM.

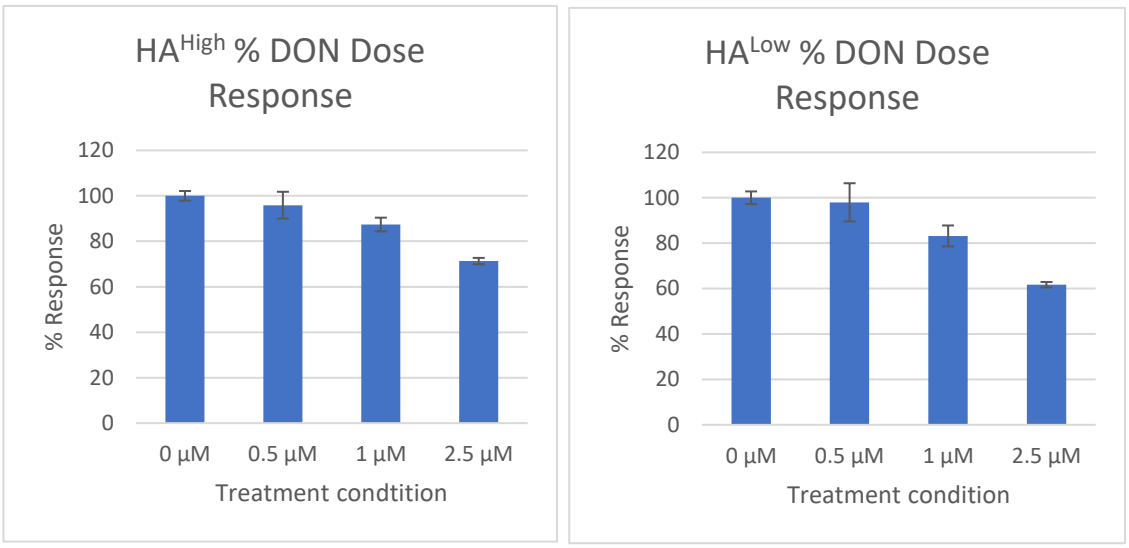

Figure 3. Percent Response for 0 µM, 0.5 µM, 1 µM, 2.5 µM DON treatments for 72h. Cells were plated on 24-well dishes at 7,000 cells/ml density and treated with for 0 µM, 0.5 µM, 1 µM, 2.5 µM DON for 72 hours, stained with crystal violet. Absorbance at 590nm was measured using Victor microplate reader. Data represent the percentage of the absorbance assessed by Victor microplate reader in each DON treatment with the control (0 nM). Mean ± SD of three replicates and are representative of at least three independent experiments.

Effects of DON on HA production of the subclones

Flow cytometry was performed to characterize the effects of DON on HA production of the subclones (***Figure 4***). For this experiment, a higher dose of DON (10 µM) was utilized at a shorter time point (48 hour). DON reduced cell-associated HA on HA^{High} cells (16.1% decrease of HABP (+) at 10 µM DON). This decrease in the expression of cell-associated HA was not observed in the HA^{Low} subpopulation treated with DON.

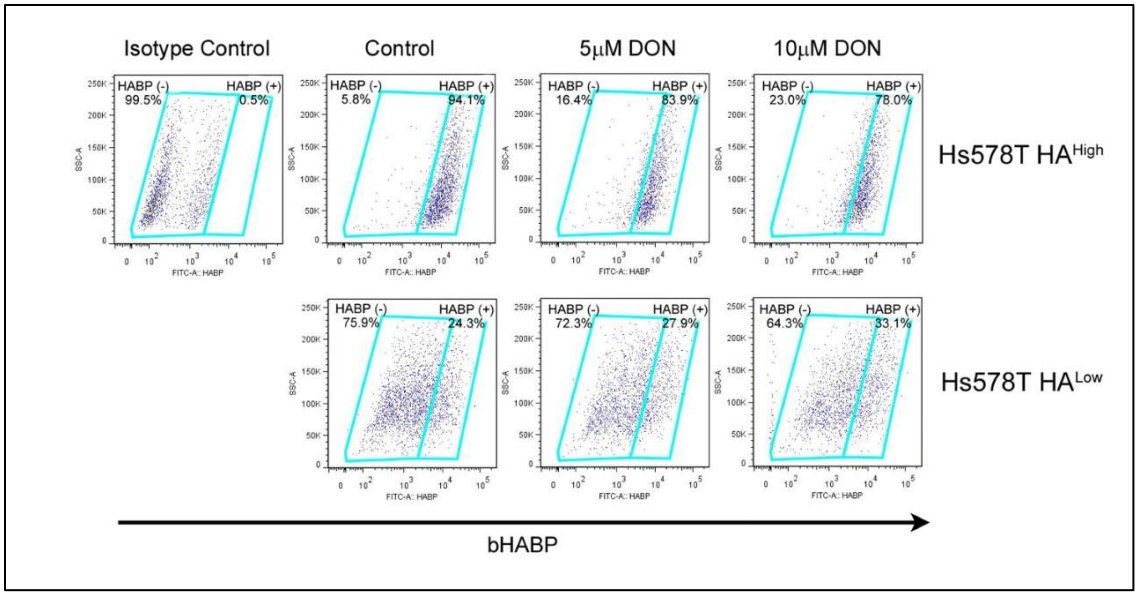

Figure 4. Flow cytometry data of bHABP binding to cell-associated HA on subpopulations incubated with 5 and 10 μM DON for 48 hours. The subclones were incubated in respective treatments, trypsinized and pooled. The pooled cells were blocked, incubated with biotinylated HA binding protein, and fluorescently labeled. Flow cytometry was performed using BD LSR II Flow Cytometer and analyzed using FlowJo 7.6.5.

Effects of DON on glycolytic function in Hs578T subclones

We also performed Glycolysis Stress Tests of Hs578T subclones pretreated 24h with 5 μM DON. The Glycolysis Stress Test measures key parameters of glycolytic function (***Figure 5A***) by directly measuring the extracellular acidification rate (ECAR) of live cells before and after serial injections of glucose, oligomycin (ATP synthase inhibitor) and 2-deoxy-glucose (2-DG, a glucose analog that inhibits glycolysis through competitive binding to hexokinase).

Glycolysis Stress Tests were conducted with Hs578T subclones after treatment with 5 μM DON for 24 hours. In ***Figure 5B***, ECAR profiles showed significant decreases in both glycolytic rate and glycolytic capacity of HA^{High} and HA^{Low} cells after 5 μM DON treatment. In HA^{Low} cells, glycolysis rate after glucose addition for untreated cells was 17.96, while that of DON treated cells was 10.34. The glycolytic capacity of untreated HA^{Low} cells was 24.43, while that of DON treated cells was 17.20. In HA^{High} cells, the glycolytic rate after glucose addition for

untreated cells was 12.98, while that of treated cells was 5.43; the glycolytic capacity of untreated cells was 19.31, while the treated was 11.23. For glycolytic reserve, there was a slight increase for HA^{Low} cells treated with 5 μM DON for 24 hours, while there was a slight decrease for HA^{High} cells, relative to untreated control cells.

A.

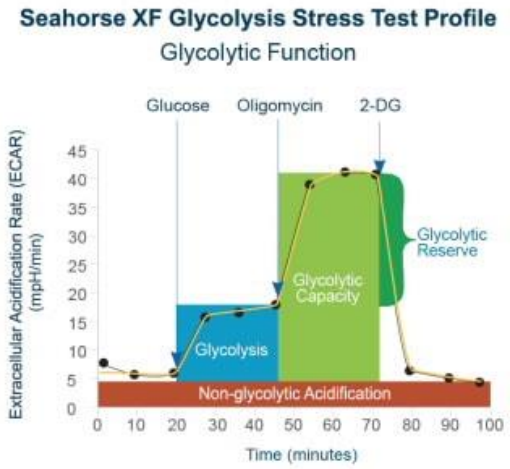

B.

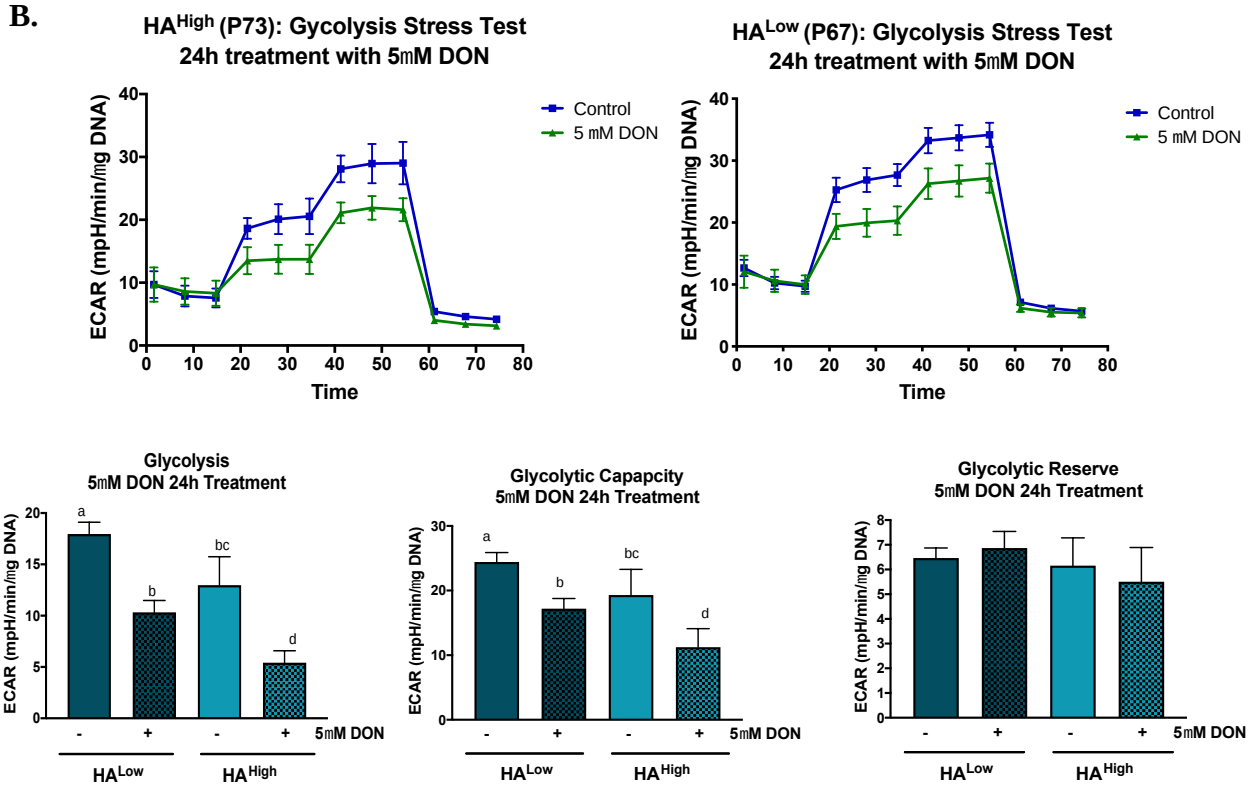

Figure 5. Effect DON on glycolytic function in live cells. HA^{High} cells were plated in Agilent Seahorse XFp cell culture microplates. The XFp flux analyzer measured temporal changes in extracellular acidification rate (ECAR) of live cells as described in Materials and Methods. A. Glycolysis Stress Test ECAR profile. B. ECAR of Hs578T subclones when treated with 5 μM DON for 24 hours. Data represents time course of ECAR before and after serial injections of of glucose, oligomycin, 2-deoxy-glucose (2-DG) and calculated parameters of glycolytic function: glycolysis, glycolytic capacity, glycolytic reserve. Data represent Mean ± SD of at least three independent biological replicates.

Effects of DON on mitochondrial respiration in Hs578T HA^{High} cells

We conducted real time metabolic flux assays on the Agilent Seahorse XFp to evaluate if HA^{High} cells exhibited altered metabolism after DON treatment. The Mito Stress Test measures key parameters of mitochondrial function (***Figure 6A***) by directly measuring the oxygen consumption rate (OCR) of live cells before and after serial injections of oligomycin (ATP synthase inhibitor), FCCP (uncoupler of oxygen consumption and ATP production), and a mix of rotenone and antimycin A (inhibitors of complex I and III, respectively).

Mito Stress Tests were conducted with HA^{High} cells in the presence 5 μM DON for 24 hours. As shown in ***Figure 6B***, OCR profiles were similar in treated and untreated HA^{High} cells, with basal and maximal OCR of approximately 20 and 30 respectively. However, DON treated HA^{High} cells exhibited a slight increase in ATP production. In addition, spare capacity was slightly reduced in HA^{High} cells after DON treatment.

A.

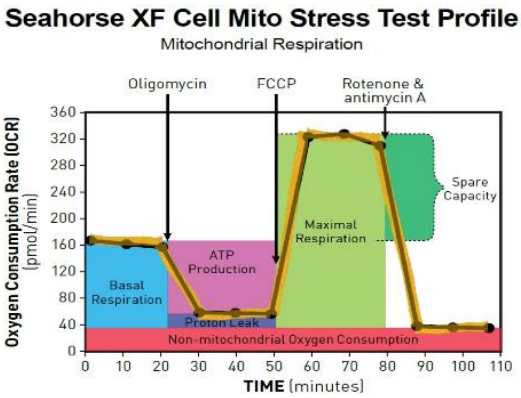

B.

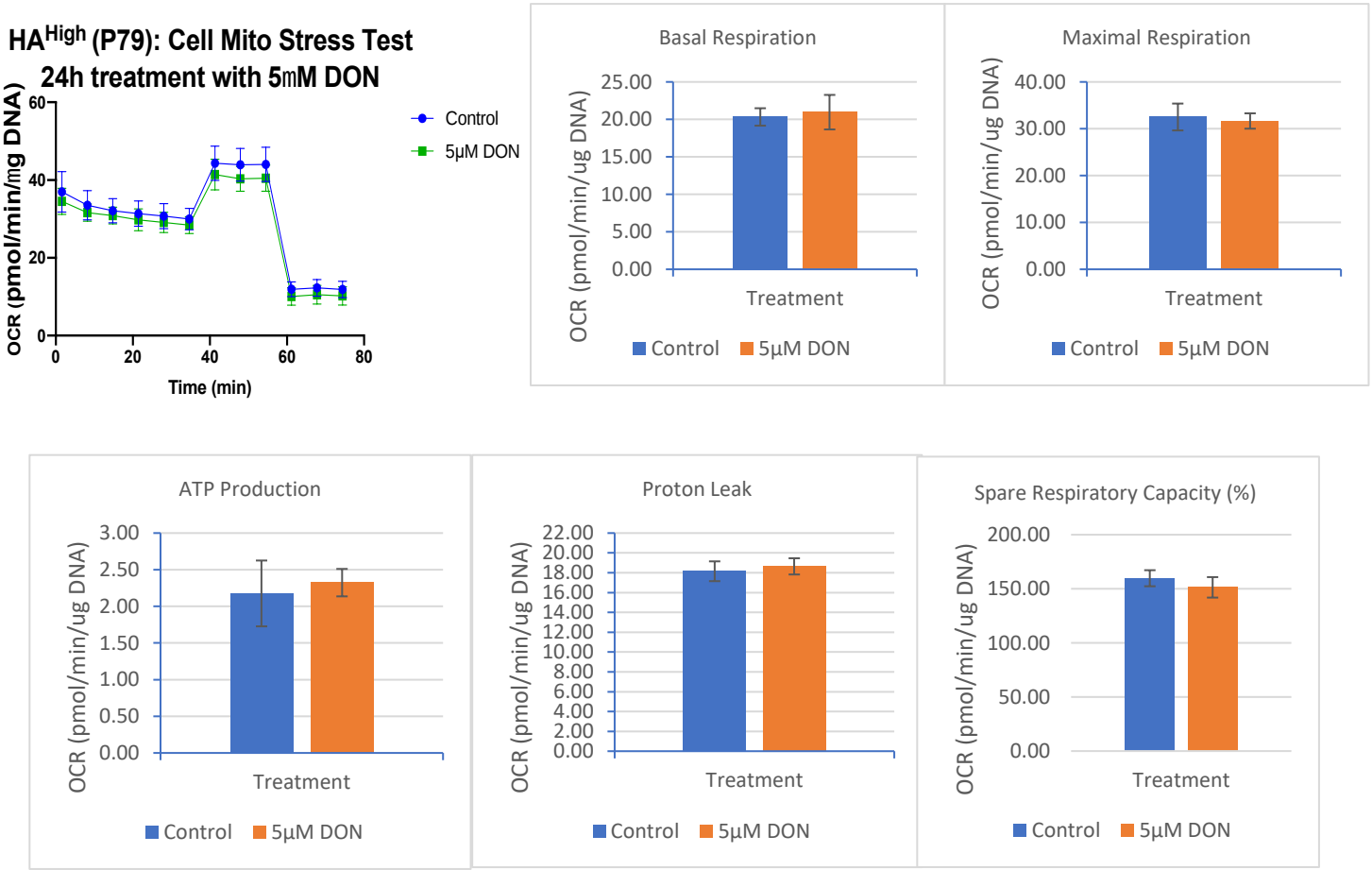

Figure 6. Effect DON on mitochondrial respiration HA^{High} cells. HA^{High} cells were plated in Agilent Seahorse XFp cell culture microplates. The XFp flux analyzer measured temporal changes in oxygen consumption rate (OCR) of live cells as described in Materials and Methods. A. Cell Mito Stress Test OCR profile. B. OCR of HA^{High} cells when treated with 5 µM DON for 24 hours. Top: Data represents time course of OCR before and after serial injections of oligomycin, FCCP and rotenone/antimycin and calculated parameters of mitochondrial respiration: basal respiration, maximal respiration, ATP production, proton leak, and % spare capacity. Data represent Mean ± SD of at least three independent biological replicates.

Discussion

We examined the HA^{High} and HA^{Low} subpopulations from basal-like TNBC Hs578T cells and found that HA^{High} cells exhibit a more aggressive phenotype with increased proliferation, enhanced HA secretion and extensive pericellular HA coat. The glutamine analog DON significantly reduced growth of both subclones at concentrations of 1.0 μM and above. Concentrations of DON of 5-10 μM were used at shorter time points for additional experiments on HA production and metabolism. At these concentrations, DON reduced cell-associated HA (as measured by flow cytometry of bHABP) in a dose dependent manner in HA^{High} cells but had no effect on HA^{Low} cells. We also examined the effect of DON on glycolysis and respiration of live cells in real time using the Seahorse metabolic analyzer. Our data demonstrated that DON inhibited glycolysis (measured as ECAR) of both clones, but HA^{High} cells were more sensitive than HA^{Low} cells. In contrast, DON did not alter mitochondrial respiration, measured as OCR, in HA^{High} cells. Thus, the effect of DON on Hs578T cell growth likely reflects its ability to block glycolysis rather than mitochondrial respiration. Further studies are warranted to determine the link between HA and glycolysis in this model system.

This project supports the concept of targeting HA synthesis as a therapeutic approach, since HA and its degradative enzymes play a central role in promoting tumorigenesis and progression of disease (Lokeshwa et al., 2014; Seufferlein et al., 2018; Yahya et al., 2014). DON, as a glutamine antagonist, targets GFAT, the key regulator in HBP and reduces HA production. In addition, DON blocks glutamine utilization for other cellular needs such as DNA synthesis. Evidence suggests that, in general, basal-like TNBC cells are more glutamine dependent than other breast cancer subtypes and thus insufficient endogenous glutamine synthesis blocks their survival (Kim et al., 2013; Oliveira et al., 2013). In our study, we observed

that cells that produce more HA (HA^{High} cells) exhibited the more aggressive phenotype and were more sensitive to DON treatment with respect to inhibition of growth and glycolysis.

The therapeutic potential of DON, however, may be impeded by its dose-limiting toxicity, specifically gastrointestinal related (Earhart et al., 1990; Magill et al., 1957; Rahman et al., 1985). Despite the potential side effects, the promising effects of DON on glutamine dependent tumors support the development of strategies to utilize it clinically for TNBC while minimizing its toxicity to normal tissues.

Conclusion

This project examined the effects of the glutamine analog DON on growth and metabolism of Triple Negative Breast Cancer cells in the context of HA synthesis. We examined the morphology of HA^{High} and HA^{Low} subpopulations and showed that the high HA producing subclone (HA^{High}) displayed a more aggressive phenotype with an extensive pericellular HA coat. Treatment with DON significantly reduced cell growth of both subclones but selectively decreased surface HA only in HA^{High} cells. Real time metabolism assays showed that treatment with 5 μM DON for 24 hours significantly altered glycolysis but not mitochondrial respiration. Furthermore, we found that glycolytic metabolism of the HA^{High} cells was more sensitive to DON treatment than the HA^{Low} cells. These findings support the concept that high HA synthesis in TNBC may increase glutamine dependency. Thus, glutamine antagonists such as DON may provide a new approach to slow TNBC growth through inhibition of HA synthesis.

References

Chokchaitaweesuk, C., Kobayashi, T., Izumikawa, T., & Itano, N. (2019). Enhanced hexosamine metabolism drives metabolic and signaling networks involving hyaluronan production and O-GlcNAcylation to exacerbate breast cancer. *Cell Death & Disease*, *10*(11), 803. https://doi.org/10.1038/s41419-019-2034-y

De Giorgi, U., Rosti, G., Frassineti, L., Kopf, B., Giovannini, N., Zumaglini, F., & Marangolo, M. (2007). High-dose chemotherapy for triple negative breast cancer. *Annals of Oncology*, *18*(1), 202–203. https://doi.org/10.1093/annonc/mdl306

Earhart, R. H., Amato, D. J., Chang, A. Y.-C., A., Borden, E. C., Shiraki, M., Dowd, M. E., Comis, R. L., Davis, T. E., & Smith, T. J. (1990). Phase II trial of 6-diazo-5-oxo-L-norleucine versus aclacinomycin-A in advanced sarcomas and mesotheliomas. *Investigational New Drugs*, *8*(1). https://doi.org/10.1007/BF00216936

Feoktistova, M., Geserick, P., & Leverkus, M. (2016). Crystal violet assay for determining viability of cultured cells. *Cold Spring Harbor Protocols*, *2016*(4). https://doi.org/10.1101/pdb.prot087379

Foulkes, W. D., Smith, I. E., & Reis-Filho, J. S. (2010). Triple-negative breast cancer. *New England Journal of Medicine*, *363*(20), 1938–1948. https://doi.org/10.1056/NEJMra1001389

Kim, S., Kim, D. H., Jung, W.-H., & Koo, J. S. (2013). Expression of glutamine metabolism-related proteins according to molecular subtype of breast cancer. *Endocrine-Related Cancer*, *20*(3), 339–348. https://doi.org/10.1530/ERC-12-0398

Lokeshwar, V. B., Mirza, S., & Jordan, A. (2014). Targeting hyaluronic acid family for cancer Chemoprevention and Therapy. *Advances in Cancer Research*, *123*, 35–65. https://doi.org/10.1016/B978-0-12-800092-2.00002-2

Magill, G. B., Myers, W. P., Reilly, H. C., Putnam, R. C., Magill, J. W., Sykes, M. P., Escher, G. C., Karnofsky, D. A., & Burchenal, J. H. (1957). Pharmacological and initial therapeutic observations on 6-diazo-5-oxo-1-norleucine (DON) in human neoplastic disease. *Cancer*, *10*(6), 1138–1150. https://doi.org/10.1002/1097-0142(195711/12)10:6<1138::aid-cncr2820100608>3.0.co;2-k

Oliveira, I. A., de Queiroz, R. M., Piva, B., Bouchuid Catão, F., da Costa Rodrigues, B., da Costa Pascoal, A., Diaz, B. L., Todeschini, A. R., Caarls, M. B., & Dias, W. B. (2019). Hexosamine biosynthetic pathway and glycosylation regulate cell migration in melanoma cells. *Frontiers in Oncology*, *9*, 116. https://doi.org/10.3389/fonc.2019.00116

Ortlund, E., Lacount, M. W., Lewinski, K., & Lebioda, L. (2000). Reactions of *pseudomonas* 7A glutaminase-asparaginase with diazo analogues of glutamine and asparagine result in unexpected covalent inhibitions and suggests an unusual catalytic triad Thr-Tyr-Glu. *Biochemistry*, *39*(6), 1199–1204. https://doi.org/10.1021/bi991797d

Perou, C. M. (2011). Molecular stratification of triple-negative breast cancers. *The Oncologist*, *16*(S1), 61–70. https://doi.org/10.1634/theoncologist.2011-S1-61

Rahman, A., Smith, FrederickP., Luc, P.-VanT., & Woolley, PaulV. (1985). Phase I study and clinical pharmacology of 6-diazo-5-oxo-L-norleucine (DON). *Investigational New Drugs*, *3*(4), 369–374. https://doi.org/10.1007/BF00170760

Seufferlein, T., Ducreux, M., Hidalgo, M., Prager, G., & Cutsem, E. V. (2018). More than a gel & hyaluronic acid, a central component in the microenvironment of pancreatic cancer. *European Oncology & Haematology*, *14*(1), 40. https://doi.org/10.17925/EOH.2018.14.1.40

Sharma, N. S., Gupta, V. K., Garrido, V. T., Hadad, R., Durden, B. C., Kesh, K., Giri, B., Ferrantella, A., Dudeja, V., Saluja, A., & Banerjee, S. (2019). Targeting tumor-intrinsic hexosamine

biosynthesis sensitizes pancreatic cancer to anti-PD1 therapy. *Journal of Clinical Investigation*, *130*(1), 451–465. https://doi.org/10.1172/JCI127515

Tamada, Y., Takeuchi, H., Suzuki, N., Aoki, D., & Irimura, T. (2012). Cell surface expression of hyaluronan on human ovarian cancer cells inversely correlates with their adhesion to peritoneal mesothelial cells. *Tumor Biology*, *33*(4), 1215–1222. https://doi.org/10.1007/s13277-012-0369-4

Vigetti, D., Deleonibus, S., Moretto, P., Karousou, E., Viola, M., Bartolini, B., Hascall, V. C., Tammi, M., De Luca, G., & Passi, A. (2012). Role of UDP- *N* -Acetylglucosamine (GlcNAc) and *O* -GlcNAcylation of Hyaluronan Synthase 2 in the control of chondroitin sulfate and hyaluronan synthesis. *Journal of Biological Chemistry*, *287*(42), 35544–35555. https://doi.org/10.1074/jbc.M112.402347

Warburg, O., Wind, F., & Negelein, E. (1927). The metabolism of tumors in the body. *The Journal of General Physiology*, *8*(6), 519–530. https://doi.org/10.1085/jgp.8.6.519

Wellen, K. E., & Thompson, C. B. (2010). Cellular metabolic stress: Considering how cells respond to nutrient excess. *Molecular Cell*, *40*(2), 323–332. https://doi.org/10.1016/j.molcel.2010.10.004

Wu, F., Lukinius, A., Bergström, M., Eriksson, B., Watanabe, Y., & Långström, B. (1999). A mechanism behind the antitumour effect of 6-diazo-5-oxo-l-norleucine (DON): Disruption of mitochondria. *European Journal of Cancer*, *35*(7), 1155–1161. https://doi.org/10.1016/S0959-8049(99)00099-4

Yahya, R., El-Bindary, A., El-Mezayen, H., Abdelmasseh, H., & Eissa, M. (2014). Biochemical evaluation of hyaluronic acid in breast cancer. *Clinical Laboratory*, *60*(7), 1115-1121. https://doi.org/10.7754/Clin.Lab.2013.130413

Yoshioka, K., Takehara, H., Okada, A., & Komi, N. (1992). Glutamine antagonist with diet deficient in glutamine and aspartate reduce tumor growth. *The Tokushima Journal of Experimental Medicine*, *39*(1–2), 69–76.